WCTE 2018
2018 World Conference on Timber Engineering
August 20 - 23, 2018 | Seoul, Republic of Korea

CAPACITY AND RELIABILITY OF LVL BEAMS MANUFACTURED FROM JUVENILE HARDWOOD PLANTATION LOGS

Benoit P. Gilbert[1], Henri Bailleres[2], Hao Zhang[3], Robert L. McGavin[4]

ABSTRACT: This paper summarises parts of the research outcomes of a university-government collaborative project aiming at determining the capacity and reliability of veneer-based structural products manufactured from early to mid-rotation (juvenile) hardwood plantations logs. Two species planted for solid timber end-products (*Eucalyptus cloeziana* and *Corymbia citriodora*) and one species traditionally grown for pulpwood (*Eucalyptus globulus*) were studied for the manufacture of the new products. Focus of this paper is on LVL beams. To cost-effectively determine the nominal design bending strengths of the new beams, a numerical model was developed. The model was found to accurately predict the strength of LVL beams with an average predicted to experimental ratio of 1.00 with a low coefficient of variation of 0.10. Using an established probabilistic database of the material properties of the veneered resources as model input, Monte-Carlo simulations were then performed. The design strength of the new LVL beams was established and found to be comparable to, and in some cases up to 2.5 times higher than, the ones of commercially available softwood products. Recommendations are also made in the paper on the appropriate capacity factors to be used for various service categories of structures. The proposed capacity factors were found to be 5% to 12% lower than the ones currently used in Australia for beams manufactured from mature softwood logs.

KEYWORDS: Juvenile hardwood, Veneer-based products, LVL beams, Numerical modelling

1 INTRODUCTION

When a manufacturer introduces new veneer-based timber structural products on the market, a costly experimental program must be undertaken. This aims at accurately measuring the strength and stiffness variations of the new products and ultimately determining their design properties. To reach a specific final product, an inefficient trail-and-error approach may be needed.

Nevertheless, expected strength and stiffness distributions of new products can be cost-effectively predicted if a methodology is developed that combines classical elastoplastic constitutive equations with a probabilistic strength prediction model of the wood veneers [1]. The veneer strength prediction model is based on characteristics which can be measured in line and the size of the veneers. This approach is followed by the authors to determine the expected structural properties of veneer-based products manufactured from early to mid-rotation (juvenile) subtropical hardwood plantation logs [2-4].

These small diameter logs currently have little to no commercial value in Australia. Nevertheless, it has been proven that they result in high grade veneer-based structural products [5, 6]. However, actual design properties were not evaluated, and because of the high proportion of defects in the resource (knots, gum veins, grain deviation ...), the new products are expected to have larger variability in their mechanical properties than commercially available products.

This paper quantifies the capacity and reliability of Laminated Veneer Lumber (LVL) beams manufactured from veneers recovered from early to mid-rotation hardwood plantation logs of two species planted for solid timber end-products (Gympie messmate (GMS) - *Eucalyptus cloeziana* and spotted gum (SPG) - *Corymbia citriodora*) and one species traditionally grown for pulpwood (southern blue gum (SBG) - *Eucalyptus globulus*). The principles behind a numerical model developed to predict the bending strength of LVL beams are introduced. Using an established probabilistic database of the tensile and compressive properties of the GMS, SPG and SBG veneers [2] as model input, Monte-Carlo simulations were performed. The design strengths of various LVL beans manufactured from juvenile hardwood plantation logs of the three species were then predicted. Appropriate capacity factors to be used for various service categories of structures are also discussed in the paper.

2 MODEL FRAMEWORK

The models for sawn timber and Glulam beams described in Buchanan [7] and Foschi and Barrett [8], respectively,

[1] Benoit P. Gilbert, School of Engineering and Built Environment, Griffith University, Australia, b.gilbert@griffith.edu.au
[2] Henri Bailleres, Salisbury Research Facility, Queensland Government, Australia, henri.bailleres@daf.qld.gov.au
[3] Hao Zhang, School of Civil Engineering, The University of Sydney, Australia, hao.zhang@usyd.edu.au
[4] Robert L. McGavin, Salisbury Research Facility, Queensland Government, Australia, robbie.mcgavin@daf.qld.gov.au

were adapted by the authors to LVL beams [3]. These models were chosen for (i) their simplicity to implement without the need of using finite element analysis (FEA) software, (ii) accuracy and (iii) rational failure criteria which reflects the actual behaviour of timber structural members for which the bending strength is higher than the tensile one [9]. The model is combined with a probability strength prediction model of the wood veneers. The main characteristics of the model are summarised below while the full model implementation is detailed in [3]

2.1 PROBABILITY STRENGTH PREDICTION OF INDIVIDUAL VENEERS

2.1.1 General

Manufacturers typically predict the strength of timber elements from characteristics which can be measured in line, such as density, Modulus of Elasticity (MOE) or knot locations. The expected strength $R_{d,predicted}$ of the element is calculated from a best fitted equation f as,

$$R_{d,predicted} = f\left(c_1, c_2, ..., c_k\right) \quad (1)$$

where c_i is the i^{th} measured characteristic and k is the total number of measured characteristics. Due to wood being a natural material, a variation exists between the actual (or measured) strength of the element and its predicted value from Eq. (1). For a given resource, this variation is expressed in term of the probability distribution function (PDF) h (or cumulative distribution function (CDF) H) for the random variable corresponding to the actual to predicted strength ratio ($R_{d,actual}/R_{d,predicted}$). The mean of the random variable is expected to be 1.0. The strength of a timber element can then be probabilistically determined from its measured characteristics as,

$$R_{d,actual} = f\left(c_1, c_2, ..., c_k\right) H^{-1}\left(P\right) \quad (2)$$

where H^{-1} is the inverse CDF (also referred to as "quantile function") and P a random number in [0, 1].

2.1.2 Characteristics c_i and veneer grading

All or parts of in line measured characteristics c_1 to c_k are typically used to grade timber elements and sort them into bins. For veneer-based products, veneers are randomly taken from one or more bins to manufacture a given grade of final product. For a given resource, the distributions of c_1 to c_k are known from accumulated past data. Let's term g_i the PDF of characteristic c_i and let's assume that in the j^{th} bin c_i ranges in $[C_{ij,L}, C_{ij,U}[$. The PDF g_{ij} of c_i in Bin j is given by the conditional PDF of g_i as,

$$g_{ij}\left(c_i\right) = \frac{g_i\left(c_i \middle| c_{ij,L} \le c_i < c_{ij,U}\right)}{\int_{c_{ij,L}}^{c_{ij,U}} g_i\left(c_i\right) dc_i} \quad (3)$$

The value of characteristic c_i of a veneer randomly taken from Bin j can then be obtained from the inverse CDF G_{ij}^{-1} as,

$$c_i = G_{ij}^{-1}\left(P\right) \quad (4)$$

where P is a random number in [0, 1].

2.1.3 Size effect

The strength of a timber element is well known to be sensitive to its size [10]. This phenomenon is commonly referred to as "size effect" [11] and is most noticeable for tensile and bending brittle failure modes [1]. Yet, timber elements failing in a ductile compressive mode are also known to be sensitive to size effects, but to a lower degree [10, 12]. Therefore, the strength of wood veneers predicted in Eq. (1) is only valid for the tested volume from which it was determined [1] and must be adjusted to reflect the volume of the veneer in a final veneer-based product. The weakest link theory [13] is well accepted in timber structures to perform this adjustment [11, 14] in both tension and compression loading [14].

Let's assume that the strength R_{d1} of a veneer predicted by Eqs. (1, 2) was obtained at a volume $V_1 = L_1 \times W_1 \times H_1$ (with the grain parallel to the longitudinal direction L), the strength R_{d2} of the same veneer at volume $V_2 = L_2 \times W_2 \times H_2$ can be deduced from the weakest link theory as [11],

$$R_{d2} = \left(\frac{L_1}{L_2}\right)^{1/k_{//}} \left(\frac{W_1}{W_2}\right)^{1/k_{\perp}} \left(\frac{H_1}{H_2}\right)^{1/k_{\perp}} R_{d1} \quad (5)$$

where $k_{//}$ and $k_{\perp}$ are the shape factors related to the dimension(s) parallel and perpendicular to the grain, respectively.

The shape factors used for each species analysed herein were determined from experimental testing [2] and the literature (see [3] for more details). Value of $k_{//}$ and $k_{\perp}$ for all analysed species are given in Table 1.

Table 1: *Shape factors for all species*

Species	Tension			Compression		
	$k_{species}$	$k_{//}$	$k_{\perp}$	$k_{species}$	$k_{//}$	$k_{\perp}$
SPG	7.4	7.4	3.7	15.6	15.6	7.8
SBG	6.5	6.5	3.2	11.7	11.7	5.9
GMS	8.5	8.5	4.2	16.1	16.1	8.1

2.1.4 Load effect

The dimensions $L_2 \times W_2 \times H_2$ of each ply to be used in Eq. (5) must also consider the actual stress distribution in the beam [11]. Let's consider a beam of dimensions $L_b \times W_b \times H_b$ and loaded in four-point bending, as shown in Figure 1, where L_{b1} is the distance between the supports and the points of application of the loads and L_{b2} the distance between loads. The length L_2 of the ply to be used in Eq. (5) is calculated from the Weibull weakest link theory [13] and is equal to [7],

$$L_2 = L_{b2} + \frac{2L_{b1}}{k_{//} + 1} \quad (6)$$

For the width and as the stress in the plies does not vary along the beam width, the width W_2 of each ply in Eq. (5) is equal to W_b for flat bending and the ply thickness for edge bending.

For the height and while the stress in the plies varies with the beam height, this variation is not considered in Eq. (5) but in the failure criteria, as detailed in Section 2.3. In Eq. (5), the height of each ply H_2 is therefore

taken as the ply thickness for flat bending and H_b for edge bending.

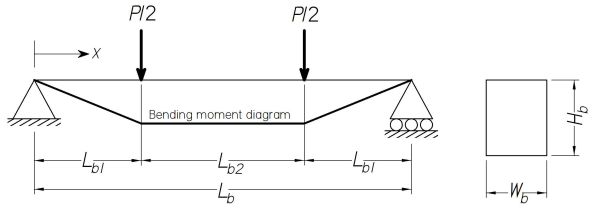

Figure 1: *LVL beam in four-point bending*

2.2 STRESS-STRAIN MODELS

The model makes use of tri-linear and linear stress-strain curves in compression and tension, respectively. The tri-linear curve in compression is given in [3] and is based on experimental material testing. This curve includes a strain softening branch with a slope equal to 7% of the MOE.

The Euler-Bernoulli beam theory is used in the model, with plane sections remaining plane. Assuming a LVL beam in pure bending, the strain profile is considered linear and the stress profile non-linear with the stress in each ply calculated from the strain profile, the ply individual MOE and the Hooke's law. The shift in neutral axis after yielding occurring in the compression zone is considered in the model. See [3] for more details.

2.3 FAILURE CRITERIA

Timber beams typically fail when brittle failure occurs in the tension zone [7]. In extreme cases, when the tensile strength is significantly higher than the compressive one, the maximum bending moment is purely reached by the formation of a plastic hinge. Both cases are considered in the model: the latter case with the non-linear compressive stress-strain curve and the former by correctly considering the relationship between the bending stress distribution in the plies and their tensile strength [9] as developed hereafter.

2.3.1 Tensile failure in flat bending

In flat bending, and based on the Weibull weakest link theory, in which the probability of failure of the non-uniformly stressed ply is equal to the one of the uniformly stressed ply in tension, tensile failure occurs when the stress at the ply bottom extreme fibre σ_{bottom} (see Figure 2 (a)) reaches the ply tensile strength R_{d2} (obtained from Eq. (5) in reference to Section 2.1.4) multiplied by the factor $S_{bending}$ given as [3],

$$S_{bending} = \left(\frac{\left(\frac{\sigma_{top}}{\sigma_{bottom}} - 1 \right)(1+k_{\perp})}{\left(\frac{\sigma_{top}}{\sigma_{bottom}} \right)^{1+k_{\perp}} - 1} \right)^{\frac{1}{k_{\perp}}} \quad (7)$$

where σ_{top} is the stress at the ply top extreme fibre.

2.3.2 Tensile failure in edge bending

In edge bending, the non-uniform tensile stress distribution in a ply on edge bending is shown in Figure 2 (b). The factor $S_{bending}$ is derived in [7] and expressed as,

$$S_{bending} = \left(\frac{1+k_{\perp}}{D_{neutral}/H_b} \right)^{\frac{1}{k_{\perp}}} \quad (8)$$

where $D_{neutral}$ is the distance from the bottom of the beam to the neutral axis.

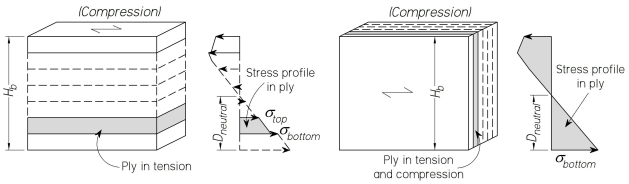

(a) *(b)*

Figure 2: *(a) non-linear stress profile on flat and (b) non-linear stress profile on edge*

2.3.3 Limitation of tensile strength

For small LVL beams, the tensile strength calculated from Eqs. (5, 7) or Eqs. (5, 8) reaches unrealistic high values, while in quasi-brittle materials, when the volume V→0, the strength should be finite [15]. For wood, the tensile strength can be limited, to the extreme case, to the tensile capacity of the cell walls. Especially considering that while woods differ in their mechanical properties, the properties of the cell walls are roughly similar for all types of wood [16], in the order of 200 to 400 MPa [16, 17].

In this study, through model calibration on LVL manufactured from SPG, it was found that the tensile strength at the extreme fibre of a ply (calculated from Eq. (5, 7) or Eq. (5, 8)) cannot be higher than twice the tensile strength of the SPG veneers obtained in [2] at a nominal reference volume V_{ref} = 500 mm × 150 mm × 7.5 mm (see also Section 3) [3].

As detailed in [3] and assuming there exists a minimum volume V_{min} for which the tensile strength of the veneer is equal to the tensile strength of the cell walls, the limiting factor $LF_{Species}$ of any analysed species can then be deduced from the limitation factor LF_{SPG} = 2.0 of the SPG species as,

$$LF_{Species} = \left(LF_{SPG}\right)^{k_{SPG}/k_{Species}} \quad (9)$$

where k_{SPG} and $k_{Species}$ are the volume shape factors of the SPG and other analysed species calculated from the tests performed in [2] and Table 1. The limiting factors are found to be equal to 1.83 and 2.39 for the GMS and SBG species, respectively.

2.4 MODEL LIMITATIONS

The veneers are assumed to be as long as the LVL beams in the study and the size effects are consequently calculated considering the entire length of the beam. The effect of the joints between veneers on the bending strength will need to be incorporated in the model.

3 VENEER PROPERTIES

3.1 STRENGTH PREDICTION

The compressive strength of the GMS, SPG and SBG veneers was determined in [2] from two characteristics c_1 and c_2 which can be measured in line during

manufacturing, namely the veneer dynamic MOE and its total knot area ratio (tKAR) [18]. The general strength best fit prediction in Eq. (1) is expressed in the form [2],

$$R_{d,predicted} = \alpha \cdot MOE^{\beta}\left(1-\gamma \cdot tKAR\right) \qquad (10)$$

where coefficients α, β and γ are given in Table 2 for each species. Note that for each species, Eq. (10) was determined from tests performed on 90 veneer sheets. Each sheet was cut into three strips which were glued together to manufacture 3-ply LVL test samples. Samples of nominal dimensions L_1 = 630 mm × W_1 = 100 mm × H_1 = 7.5 mm and L_1 = 500 mm × W_1 = 150 mm × H_1 = 7.5 mm were used for compressive and tensile testing, respectively. A two-parameter Weibull distribution was found to best fit the CDF H of the random variable corresponding to the actual to predicted strength ratio ($R_{d,actual}/R_{d,predicted}$) in the form,

$$H\left(\frac{R_{d,actual}}{R_{d,predicted}}\right) = 1-e^{-\left(\frac{R_{d,actual}}{\lambda R_{d,predicted}}\right)^{k_{species}}} \qquad (11)$$

where the shape factors $k_{species}$ are given in Table 1 and the scale parameters λ in [2].

Table 2: *Shape factors for all species*

Species	Tension			Compression		
	α	β	γ	α	β	γ
SPG	0.025	0.842	1.110	0.490	0.506	0.437
SBG	0.117	0.694	1.575	0.810	0.437	0.246
GMS	0.013	0.896	1.211	0.680	0.474	0.388

3.2 GRADING AND CHARACTERISTICS

Three different veneer grades, defined in [2], are used herein. The grades only use the veneer MOE value as the sole grading indicator. The MOE cut-off values between each grade are given in [2] and are based on the expected distributions of MOE encountered in a mill [19]. The grades divide veneers into three bins, each with an equal number of veneers, and mimic a simple way a manufacturer could divide the veneers. The grades are referred to as "Low" (L), "Medium" (M) and "High" (H), in increasing value of the MOE.

The distribution of the dynamic veneer MOE (characteristic c_1) has been quantified in [19] for the resources analysed. This characteristic is modelled in this paper through a Weibull distribution and its overall CDF G_1 is in the form,

$$G_1\left(MOE\right) = 1-e^{-\left(\frac{MOE}{\lambda_1}\right)^{k_1}} \qquad (12)$$

where k_1 and λ_1 are given in [4] for all species.

The distribution of the expected tKAR value of a veneer of length L (characteristic c_2) is defined in [2]. For each grade, a Weibull distribution was also found to best fit the distribution of the tKAR values. The CDF G_{2j} for characteristic c_2 in Bin j (j = [L, M, H]) is in the form (see [2] for more details),

$$G_{2\,j}\left(1-tKAR\right) = 1-e^{-\frac{L}{L_{ref}}\left(\frac{1-tKAR}{\lambda_{2\,j}}\right)^{k_{2\,j}}} \qquad (13)$$

where L_{ref} = 150 mm. k_{2j} and λ_{2j} are given in [2] for all species and grades.

4 MODEL CALIBRATION AND VALIDATION

The model was calibrated in [3] against four-point flat and edge bending tests performed on five different 7- and 8-ply LVL samples, all manufactured from SPG veneers. The model was then validated against the four-point flat and edge bending tests performed in [5] on (i) eight 13-ply LVL samples manufactured from SPG veneers and (ii) eight 13-ply LVL samples manufactured from GMS veneers. The details of the experimental tests and construction strategies for all panels are given in [3, 5]. Note that in [3], the MOE, tensile strength and compressive strength of each veneer within the manufactured LVL were experimentally assessed. In [5], only the veneer MOE of each ply was measured prior to the LVL manufacture.

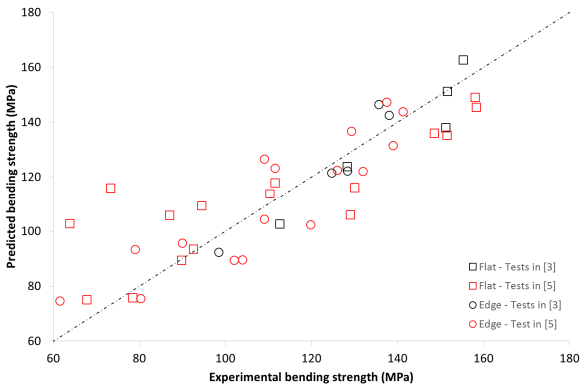

Figure 3: *Strength comparison experimental versus numerical*

Figure 3 shows the experimental versus predicted results for all test performed, both on flat and edge bending. The average predicted to experimental ratios are equal to 0.98 and 1.01 for flat and edge bending, respectively. Both flat and edge bending have an associated Coefficient of Variation (CoV) of 0.10. See [3] for more details on the results and obtaining the average predicted to experimental ratios and CoV.

The model is also able to well reproduce the non-linear response of the beams. Figure 4 compares the flat bending experimental to predicted responses of two different samples.

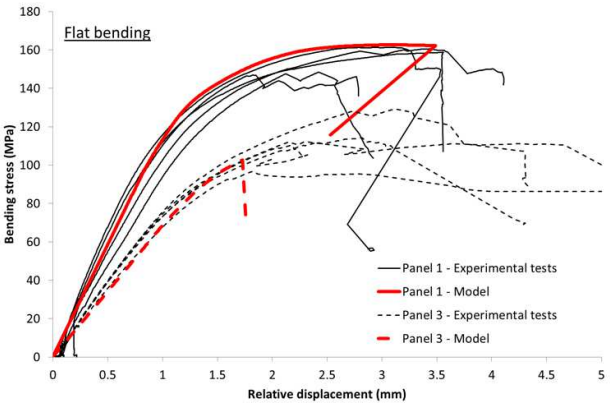

Figure 4: *Response comparison experimental versus numerical*

5 CAPACITY OF THE NEW PRODUCTS

5.1 General

The expected bending strength distributions of six commercially available LVL beam sizes, manufactured from early to mid-rotation GMS, SPG and SBG hardwood plantation veneers, were investigated using the validated numerical model. The beams are manufactured from 3.0 mm thick veneers and are (i) 15-ply (45 mm thick) of height of 200 mm, 300 mm and 400 mm, and (ii) 21-ply (63 mm thick) of height of 240 mm, 400 mm and 600 mm. Four different construction strategies are investigated:

- Low (L): the beams are solely manufactured from the "Low" grade veneers (refer to Section 2.1.2 for grade definition).
- Medium (M): the beams are solely manufactured from the "Medium" grade veneers.
- High (H): the beams are solely manufactured from the "High" grade veneers.
- All (A): the beams are manufactured with an equal number of veneers from each grade, using the "Low" for the middle veneers, the "Medium" for the adjacent veneers and the "High" for the external veneers.

The expected distribution of MOE encountered for the studied veneered resources in a mill (Eq. (12)), the expected tKAR value of the veneers (Eq. (13)) and the veneer strength (Eq. (11)) were used as random model input. The detailed flowchart is given in [3]. Per studied configuration, 10,000 Monte-Carlo simulations were run. Four-point bending tests were simulated on both flat and edge following the recommendations in the Australian/New-Zealand standard AS/NZS 4357.2 [20]. The uncertainty in the numerical model in predicting the actual bending strength of the LVL beams was also considered in this parametric study. An average predicted to actual strength ratio (Mean/Nominal) of 1.00 and a CoV of 0.10 were used with an assumed normal distribution. More details can be found in [3].

5.2 Results

Figure 5 gives the strength distribution of the 200×45 LVL beams on flat bending for all strategies and species. The simulations for all remaining beams show a similar trend to the ones presented in Figure 5. The strength variability in edge bending is less than on flat bending. Table 3 shows the bending design strength, defined as the 5th percentile strength, of selected beams. Edge bending generally gives higher bending strength than flat bending for the same configuration. Using all the veneered resources in the construction strategy allows reaching bending strength (i) between the "Medium" and "High" construction strategies on flat bending and (ii) very similar to the "Medium" strategy on edge bending. Softwood LVL beams available in Australia [21, 22] have design bending strength of about 42 to 44 MPa and 38 MPa for 200 mm and 600 mm deep beams, respectively, on edge and 42 MPa on flat. Within the limitation of the model, design bending strengths, superior to the previous commercialised softwood LVL beams, are reported in Table 3. Only the SPG beams manufactured from low grade veneers have similar or lower bending strengths to the ones of the commercialised softwood beams. For all analysed species and configurations, the LVL beams manufactured from the high grade veneers have design bending strengths 1.5 to 2.5 greater than the commercialised softwood beams. On edge bending, using all veneer grades in the manufacturing gives design bending strengths ranging from 48.1 MPa for the 600×63 SPG beams to 79.2 MPa for the 200×45 GMS beams. For all flat and edge studied cases, the highest design values of 83.9 and 97.2 MPa, respectively, are both found for the 200×45 GMS beams.

Table 3: *Flat and edge bending design bending strength (5th percentile of simulations) for selected beams – in MPa*

Beam	Grade	SPG		SBG		GMS	
		Flat	Edge	Flat	Edge	Flat	Edge
200 ×45	L	43.2	52.2	53.1	61.0	47.6	58.6
	M	62.6	73.8	68.4	74.2	67.9	81.1
	H	81.6	92.6	81.7	84.2	83.9	97.2
	A	75.2	73.0	75.7	73.2	77.6	79.2
400 ×45	L	37.0	38.7	43.7	46.5	40.7	46.3
	M	53.1	56.6	56.6	58.6	57.9	65.9
	H	68.5	73.5	68.4	69.0	72.3	80.7
	A	63.7	56.4	63.4	58.9	66.2	64.6
600 ×63	L	33.7	32.3	38.2	39.4	37.1	40.4
	M	49.9	48.4	50.7	50.7	54.1	58.1
	H	62.5	63.5	59.8	60.5	65.9	71.8
	A	56.1	48.1	54.0	50.5	59.3	56.7

In general, the SPG and GMS beams have the lowest and highest design bending strength of all three analysed species.

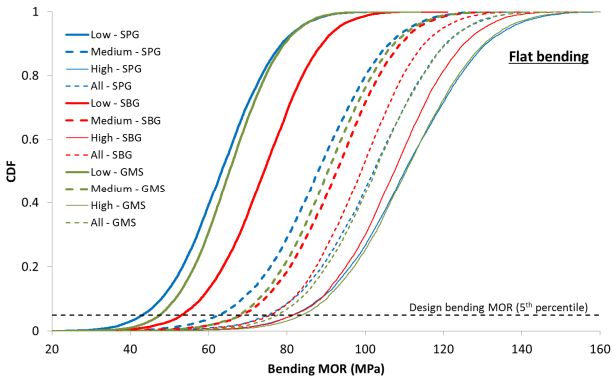

Figure 5: *Predicted strength distribution of 200×45 LVL beams*

6 RELIABILITY ANALYSIS

6.1 Framework

The relationship between the reliability index and the capacity factors, also referred to as "resistance factors", to be used in limit state design of LVL beams manufactured from early to mid-rotation subtropical GMS, SPG and SBG plantation veneers, in both edge bending and flat bending, were investigated in [23]. The analyses were conducted on the six different beam sizes

and the four grades mentioned previously. Four main load combinations (combinations of dead, live and wind loads) specified in the Australian New Zealand Standard AS/NZS 1170.0 [24] were considered as:

- *LC1*: 1.35 G_n (Dead loads only) and k = 0.57
- *LC2*: 1.2 G_n + 1.5 L_n (Dead + Sustained and Extraordinary live loads) and k = 0.80
- *LC3*: 1.2 G_n + 1.5×0.4 L_n (Dead + Sustained live loads) and k = 0.57
- *LC4*: 1.2 G_n + W_n + 0.4 L_n (Dead + Wind + Sustained live loads) and k = 1.00

where k represents the load duration factor which depends on the duration of the load combination of interest.

The load duration effects (damage accumulation) were considered in the study over the assumed 50 years life time of the structure. The model developed by Gerhards [25, 26] was used. The evolution of the degree of damage α relative to the time t is therefore given as,

$$\frac{d\alpha}{dt} = e^{-a+b\frac{f(t)}{f_0}} \quad (14)$$

where a and b are two constants found through experimental tests, f(t) is the stress at time t and f_o is the short-term strength. α = 0 means no damage and α = 1 means total damage (failure) of the timber element. Values of coefficients a and b for structural lumbers found in the literature at temperature and relative humidity close to the ambient ones are reported in [34] [42]. The smaller the values of a and b are, the more sensitive the timber is to creep deformation and the faster the structural element fails under a sustained load. The existing researches on reliability of timber structures typically use values of a and b around a = 38-40 ln(day) and b = 46-50.

To analyse the reliability of the new products in [23], three rates of damage accumulation, based on the data available in the literature, were considered.

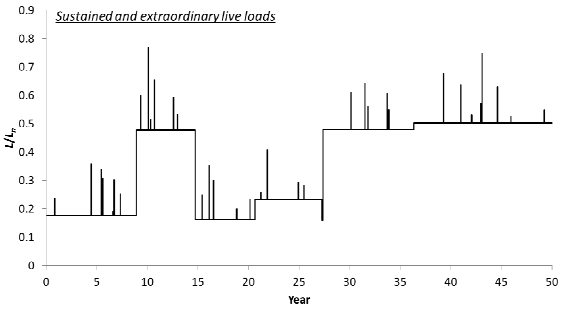

Figure 6: *Example of a stochastic Sustained and Extraordinary live loads*

The live loads were treated as a stochastic process and were broken down into two components, as in design specifications, (i) a sustained (or "arbitrary point-in-time") component L_s representing the live load due to normal use of the structure (weight of people, furniture, moveable equipment…etc.) and (ii) an extraordinary component L_e that simulates shorter events such as crowd gathering, temporary storage during remodelling or emergencies [27]. Details on the stochastic process is given in [23]. Figure 6 shows an example of live load generated in [23]. Other load models used are detailed in [23].

6.2 Recommendations

Based on Monte-Carlo simulations and using the targeted reliability indices β_T (i) specified in [28] for the different service categories of structures in the Australian standard AS 1720.1 [29] for LC1 to LC3 and (ii) of 2.5 [30] for all service categories for LC4 due to the reliability index when designing for wind load being historically lower than when designing for gravity load [30, 31], recommendations were made on the appropriate capacity factors to be used. Results show that LC2 and LC4 typically govern the choice of the capacity factor.

Table 4 gives the proposed ϕ factors for all structural service categories in the AS 1720.1 [29] following the observations presented in [23]. Contrary to international design specifications [24, 32, 33], where no difference is made between edge and flat bending in the choice of ϕ, two sets of capacity factors were proposed due the different edge and flat bending strength distributions.

The reliability factors of the proposed LVL products are 5% to 12% lower than the ones specified in the Australian standard AS 1720.1 [29] for commercialised LVL beams (typically manufactured from mature softwood logs). However, (i) stochastic load processes combined with a proper load damage accumulation model was likely not considered in the calibration of the AS 1720.1 and (ii) a different mean to nominal ratio was also likely used for the wind load [23, 34]. Ellingwood et al. [27, 35] showed that the former approach is unsafe and overestimates the reliability index β. The difference in β between the present study and the AS 1720.1 may therefore be less significant if similar reliability analysis framework were adopted. Further investigations are needed to evaluate this difference.

Table 4: *Proposed capacity factors for the LVL beams manufactured from early to mid-rotation hardwood plantation logs (Governing load combination showed in bracket)*

Product	Category 1 *Houses and secondary structures*	Category 2 *Primary structures other than houses*	Category 3 *Primary structures intended to full and essential service or post disaster function*
LVL in AS 1720.1 [29]	0.95	0.90	0.80
Proposed LVL – Edge bending	0.85 (LC4)	0.85 (LC4)	0.80 (LC2 & LC4)
Proposed LVL – Flat bending	0.85 (LC4)	0.80 (LC2)	0.70 (LC2)

7 CONCLUSION

The paper presented a numerical model to predict the strength of LVL beams. The statistical distributions of the strength of LVL beams manufactured from early to mid-rotation (juvenile) hardwood plantations logs were presented. Capacity factors to be used in limit state design equations for the new products were also proposed and found to be lower than those currently used for LVL beams manufactured from mature softwood logs.

ACKNOWLEDGEMENT

This project was supported by the Australian Research Council, under project DE140100212.

REFERENCES

[1] P.L. Clouston, F. Lam "Computational Modeling of Strand-Based Wood Composites", *ASCE Journal of Engineering Mechanics*, 127, 844-851, 2001.

[2] B.P. Gilbert, H. Bailleres, M.F. Fischer, H. Zhang, R.L. McGavin "Mechanical properties of rotary veneers recovered from early to midrotation subtropical-hardwood plantation logs for veneer-based composite applications.", *ASCE Journal of Materials in Civil Engineering*, 29, 04017194, 2017.

[3] B.P. Gilbert, H. Bailleres, H. Zhang, R.L. McGavin "Strength modelling of Laminated Veneer Lumber (LVL) beams", *Construction and Building Materials*, 149, 763-777, 2017.

[4] B.P. Gilbert "Compressive strength prediction of veneer-based structural products", *ASCE Journal of Materials in Civil Engineering (Accepted)*, 2018.

[5] R.L. McGavin, H. Bailleres, F. Lane, J. Fehrmann, High value timber composite panels from hardwood plantation thinnings, Department of Agriculture, Fisheries and Forestry, Brisbane, Australia, 2013.

[6] A. Monteiro de Carvalho, F.A. Rocco Lahr, G.J. Bortoletto "Use of brazilian eucalyptus to produce LVL panels", *Forest Products Journal*, 54, 61-64, 2004.

[7] A.H. Buchanan "Bending Strength of Lumber", *ASCE Journal of Structural Engineering*, 116, 1213-1229, 1990.

[8] R.O. Foschi, J.D. Barrett "Glued-Laminated beam strength: a model", *Journal of the structural division*, ST8, 1735-1754, 1980.

[9] S. Thelandersson, Introduction: Wood as a construction material (Chapter 2), in: S. Thelandersson, H.J. Larsen (Eds.) Timber Engineering, Wiley and Sons, England, 2003.

[10] J.D. Barrett, F. Lam, W. Lau "Size Effects in Visually Graded Softwood Structural Lumber", *ASCE Journal of Materials in Civil Engineering*, 7, 19-30, 1995.

[11] T. Isaksson, Structural timber - Variability and statistical modelling (Chapter 4), in: S. Thelandersson, H.J. Larsen (Eds.) Timber Engineering, Wiley and Sons, England, 2003.

[12] ASTM D1900-16, *Standard Practice for Establishing Allowable Properties for Visually-Graded Dimension Lumber from In-Grade Tests of Full-Size Specimens*, ASTM International, Pennsylvania, USA, 2016.

[13] W. Weibull, A statistical theory of strength of materials, Generalstabens litografiska anstalts förlag, Stockholm, 1939.

[14] B. Madsen, A.H. Buchanan "Size effect in timber explained by a modified weakest link theory", *Canadian Journal of Civil Engineering*, 13, 218-232, 1986.

[15] Z.P. Bažant, S.D. Pang, M. Vořechovsky, D. Novák, R. Pukl, "Statistical size effect in quasibrittle materials: Computation and extreme value theory." Fracture Mechanics of Concrete Structures ", *Proceedings of the 5th International Conference on Fracture Mechanics of Concrete and Concrete Structures* (Eds.: V.C. Li, K.Y. Leung, K.J. Willam, S.L. Billington), Vail, U.S.A., 189--196., 2004.

[16] L.J. Gibson, M.F. Ashby, Wood (Chapter 10), in: D.R. Clarke, S. Suresh, I.M. Ward FRS (Eds.) Cellular solids - Structure and properties - Second edition, Cambridge university press, UK, 1999.

[17] A. Krauss, W. Moliński, J. Kúdela, I. Čunderlík "Differences in the mechanical properties of early and latewood within individual annual rings in dominant pine tree (Pinus sylvestris L.) ", *Wood research*, 56, 1-12, 2011.

[18] T. Isaksson, *Modelling the variability of bending strength in structural timber - Length and load configuration effects - Report TVBK-1015*, Thesis, Lund University, Lund, Sweden, 1999.

[19] R.L. McGavin, H. Bailleres, J. Fehrmann, B. Ozarska "Stiffness and Density Analysis of Rotary Veneer Recovered from Six Species of Australian Plantation Hardwoods", *BioRessources*, 10, 6395-6416, 2015.

[20] AS/NZS 4357.2, *Structural laminated veneer lumber, Part 2: Determination of structural properties - Test methods*, Standards Australia, Sydney, Australia, 2006.

[21] Carter Holt Harvey Woodproducts, Futurebuild LVL specific engineering design guide, in, Carter Holt Harvey Woodproducts, 2015.

[22] Hyne timber, *LVL Design Information*, http://www.hyne.com.au/timber-centre/lvl/designinformation, Accessed on.

[23] B.P. Gilbert, H. Zhang, H. Bailleres "Reliability of laminated veneer lumber (LVL) beams manufactured from early to mid-rotation subtropical hardwood plantation logs", *Structural Safety*, 2018 (Submitted).

[24] AS/NZS 1170.0, *Structural design actions, Part 0: General principles*, Standards Australia, Sydney, Australia, 2002.

[25] C.C. Gerhards "Time-related effects on wood strength: a linear cumulative damage theory", *Wood Science and Technology*, 11, 139-144, 1979.

[26] C.C. Gerhards, C.L. Link "A cumulative damage model to predict load duration characteristics of lumber", *Wood and fibre science*, 19, 147-164, 1987.

[27] B.R. Ellingwood, D. Rosowsky "Duration of Load Effects in LRFD for Wood Construction", *ASCE Journal of Structural Engineering*, 117, 584-599, 1991.

[28] AS 5104, *General principles on reliability for structures*, Standards Australia, Sydney, Australia, 2005.

[29] AS 1720.1, *Timber structures, Part 1: Design methods*, Standards Australia, Sydney, Australia, 2010.

[30] B.R. Ellingwood, T.V. Galambos, J.G. MacGregor, C.A. Cornell, Development of a probability based load criterion for American National Standard A58 - Building code requirement for minimum design loads in buidlings and other structures, Washington D.C., U.S.A., 1980.

[31] B.R. Ellingwood, P.B. Tekie "Wind Load Statistics for Probability-Based Structural Design", *Journal of Structural Engineering*, 125, 453-463, 1999.

[32] ANSI/AWC NDS, *National design specification (NDS) for wood construction*, American Wood Council, Leesburg, U.S.A., 2015.
[33] EN 1995-1-1, *Eurocode 5: Design of timber structures - Part 1-1: General - Common rules and rules for buildings* The European Union Per Regulation, Brussel, Belgium, 2004.
[34] L. Pham, J. Carson "Derivation of equations for determination of capacity factors (report prepared for SAI TC TM001/WG)", *Non published*, 2007.
[35] B.R. Ellingwood "Probability-based LRFD for engineered wood construction", *Structural Safety*, 19, 53-65, 1997.